Nano World Journal

https://doi.org/10.17756/nwj.2020-074

Research Article

Open Access

ZnO Nanostructure Based Photocatalysis for Water Purification

Yamin Leprince-Wang*, Nathan Martin, Yamina Ghozlane Habba, Marie Le Pivert and Martine Capochichi-Gnambodoe

ESYCOM Lab, University Gustave Eiffel, France

*Correspondence to:
Prof. Yamin Leprince-Wang
ESYCOM Lab (CNRS UMR9007)
University Gustave Eiffel
F-77454 Marne-la-Vallée, France
Tel: +33 1 6095 7276
E-mail: yamin.leprince@u-pem.fr

Received: December 02, 2020
Accepted: February 24, 2020
Published: February 25, 2020

Citation: Leprince-Wang Y, Martin N, Habba YG, Le Pivert M, Capochichi-Gnambodoe M. 2020. ZnO Nanostructure Based Photocatalysis for Water Purification. *NanoWorld J* 6(1): 1-6.

Published by United Scientific Group

Abstract

In recent years, semiconductor based photocatalysis has shown great potential for an application as a low-cost, environmentally friendly and sustainable water treatment technology. Its efficiency has been widely demonstrated on the removal of persistent organic compounds in water. This paper studies the photocatalytic activity of ZnO nanowires (NWs) grown on a substrate, a configuration which can be considered advantageous over freely suspended nanoparticles (NPs) commonly used in many research works, due to its easy removal from purified water and reutilization. The characterization of the ZnO NWs morphology and structure was performed by scanning electron microscope (SEM) and X-ray diffraction (XRD) measurements. The photocatalytic efficiency study has been carried out by using three organic dyes (MB, MO and AR14), as commonly used pollutants in various industrial activities. For a better understanding of the photocatalytic efficiency versus the liquid regime, the photocatalysis has been carried out under classic mode and microfluidic mode. All tests shown the notable photocatalytic efficiency of ZnO NWs. Moreover, remarkable results were achieved with our ZnO-NWs-integrated microfluidic reactor, which exhibited an important enhancement of photocatalytic activity by reducing the photodegradation time from hours to minutes.

Keywords

ZnO, Nanowires, Water purification, Photocatalysis, Microfluidics

Introduction

Nowadays, the impact on environment and on human health of different pollutants, especially chemical pollutants, is becoming critical due to its drastic consequences on our main vital resource, water. The World Health Organization (WHO) has set the water quality at the top of its priority action list. Some kinds of organic pollutants, known as "persistent organic pollutants" (POPs), such as dyes, issued from textile, pharmaceutical and food-processing industries, cannot be totally degraded by using conventional wastewater treatment methods. Therefore, it is urgent and challenging to find low-cost and environmentally friendly new solutions.

In recent years, extensive efforts of fundamental research and development of practical processes have been devoted to water purification treatments. The water purification by metal oxide semiconductor, based on the photocatalytic effect, is one of the more attractive and promising methods compared to its classical counterparts such as adsorption, sedimentation, and filtration. Indeed, it is a low-cost method and it possesses the ability to decompose a wide range of organic water

pollutants into harmless products at room temperature, without the residual deposit needing further post-treatment [1, 2].

The most widely used metal-oxide as photocatalysts are titanium dioxide (TiO_2) and zinc oxide (ZnO) due to their intrinsic photocatalytic properties, thanks to their wide bandgap (> 3.2 eV) [3-5]. Over the past decades, TiO_2 has notably received much attention in photocatalytic study. However, this metal oxide has recently become a more controversial material, as it is suspected to be carcinogenic [6, 7]. Contrary to TiO_2, ZnO is nontoxic and biocompatible [8], this environmentally friendly property making it a suitable photocatalyst for water purification application. Moreover, ZnO nanostructures are interesting due to their high quantum efficiency [9], low cost and easy-controllable synthesis onto diverse substrates with ultra-high specific surface [10, 11], and chemical and thermal stability [12, 13].

However, a big challenge remaining to the use of ZnO nanostructures as photocatalysts toward water purification is the length-scale limit of the mass transfer during the degradation process of polluted water, mainly due to the short diffusion length [14, 15]. Fortunately, it is expected that microfluidic systems can provide ultra-high purity water by taking advantage of their appropriate size for reaction-diffusion process, and their easy, low-cost fabrication. By matching the flow rate and reaction-diffusion process of the ZnO nanostructures under UV illumination, a practical microfluidic system can be developed for ultra-purified water treatment.

In this work, three organic dyes, commonly used in textile, food-processing, and pharmaceutical industries, have been used for the photocatalysis study: methylene blue (MB), methyl orange (MO), and azorubine (also called acid red 14 - AR14). A systematical study has been carried out by comparing the photocatalytic efficiency between classic mode (or bulk mode) and microfluidic mode. We demonstrated that the photocatalytic efficiency has been substantially increased under microfluidic mode. The photocatalytic activity of the ZnO NWs for the organic pollutant degradation was investigated using the three aforementioned organic dyes in aqueous solution. The detailed degradation mechanism for each dye has been proposed in our previous work [16].

The morphology of the ZnO NWs was characterized using a scanning electron microscopy (FEG–SEM, NEON 40 ZEISS, Berkochen, Germany) operating at an accelerating voltage of 10 kV. The photocatalytic process was followed by an UV-Vis spectrophotometer (Lambda 35, Perkin Elmer, Waltham, MA, USA). Samples from the organic-dye-polluted water were periodically taken during the photo-degradation process, in order to monitor the evolution of the photodegradation rate by measuring their absorption spectra.

Material and Methods

ZnO nanowire synthesis

The ZnO NWs were synthesized by a low cost two-step hydrothermal method with a high aspect ratio [17], offering a large effective surface, which is beneficial for the photocatalytic process.

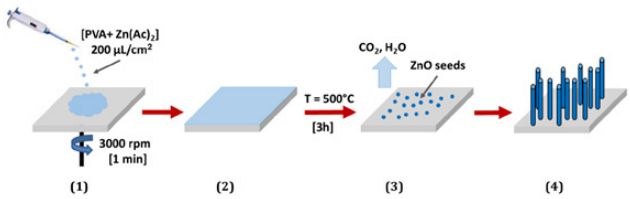

Figure 1: Drawing of the ZnO nanowire formation: (1) Seedlayer spin-coating; (2) Spin-coated seedlayer post-annealing at 500°C during 3 hours; (3) ZnO seeds (nanocristallites) formation; (4) ZnO nanowire growth at 95°C during 4 hours.

Figure 1 summarizes the synthesis process of the ZnO NWs, which was realized by a two-step hydrothermal method: the seed layer, consisting of 2 g of polyvinyl alcohol (PVA) and 0.25 g of zinc acetate dehydrate ($Zn(CH_3COO)_2.2H_2O$) dissolved in water, was firstly spin-coated on the clean substrates as described in our previous work [16], followed by an annealing at 500°C during 3 hours in order to form the ZnO nanocristallites as seeds. The ZnO NWs were then grown on the seed layer in a solution containing 25 mM of zinc nitrate ($Zn(NO_3)_2$) and 12.5 mM of Hexamethylenetetramine (HMTA) at 95°C during 4 hours. The substrate surface with ZnO nanowires is about 2 cm^2.

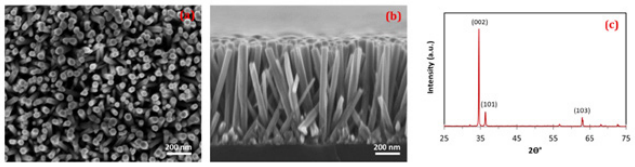

Figure 2: (a) Plan-view and (b) cross-section view SEM images showing the homogeneous morphology of the ZnO nanowire array grown on Si substrate at 95°C during 4 hours via hydrothermal method. (c) XRD spectrum of ZnO nanowire array showing a favorite growth direction towards c-axis.

The plane-view and cross-section view SEM image of the ZnO NWs showed that high aspect ratio ZnO NWs were obtained with a quite homogeneous morphology (Figures 2a and 2b). For the 4 h growth time sample, the average NW length is of ~ 850 nm and the NW diameter is of ~45 nm (for an aspect ratio of ~19). This kind of microstructures offers a large effective surface for the contact with the pollutant molecules and the light absorption, enhancing the photocatalytic efficiency. Furthermore, the X-ray diffraction (XRD) measurements showed the ZnO nanowires own the typical ZnO Würtzite structure with preferred growth direction towards the c-axis (Figure 2c). It is well known that such crystalline structure will give a better photocatalytic activity compared to other crystalline orientations [18]. In fact, the c-axis oriented ZnO NWs will favor the H_2O_2 generation, then produce more OH• radicals, which improves the photocatalytic activity, according to the semiconductor-based photocatalysis mechanism [19].

Microfluidic chamber fabrication with integrated ZnO nanowires

The microfluidic chamber fabrication is a multi-step process. First, the ZnO nanowire array is synthesized on a

classical laboratory substrate, like glass or Si wafer, via the hydrothermal method presented in the previous paragraph, thus the nanowire microstructure is the same that the one shown in figure 2. Second, the PDMS (polydimethylsiloxane) cover is prepared. To ensure the good stability and impermeability of the chamber after tubing, it must have a thickness of about 3 mm. It will also be shaped with the same dimensions as the substrate. Two holes are then pierced with a Biopsy punch (d = 0.5 mm), to let the fluid inlet and outlet tubes pass. Finally, the third step is the assembly of the chamber itself, using a gene frame to connect the substrate and the PDMS. Here, the gene frame plays the role of a spacer, which gives the microfluidic chamber a height of about 250 µm. The microfluidic chamber volume can be estimated as about 50 mm^3 with a ZnO nanowires decorated surface of about 2 cm^2, similar to the ZnO nanowires open substrate described in the previous paragraph.

Figure 3a illustrates the fabrication process of the microfluidic chamber with the integrated ZnO nanowires, and figure 3b shows an optical graph of the planar microfluidic reactor; while figure 3c details the view of the as-prepared microfluidic chamber for photocatalytic water purification. Figure 3d shows the experimental set-up, where the polluted water was pushed by a syringe pump with a flow rate of 250 µL/min.

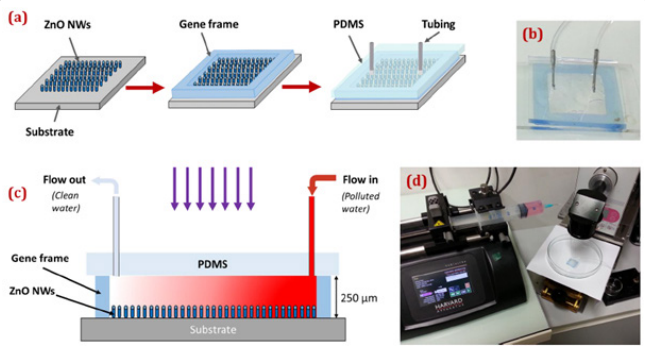

Figure 3: (a) Illustration of the microfluidic chamber fabrication with integrated ZnO NWs, and (b) photography of a completed chamber. (c) Detailed microfluidic chamber for water purification via the photocatalytic effect of ZnO NWs. (d) Experimental set-up for photocatalysis in microfluidic mode.

Results and Discussion

Photocatalysis is the phenomenon that occurs when a chemical reaction is accelerated or activated under the action of light. To be able to activate the photocatalysis, it is necessary to put the reactive species in the presence of a photocatalyst, a chemical species which will accelerate the reaction speed under the appropriate lighting but will not be modified by the reaction. In general, the compounds that can be used as photocatalysts are semiconductors. When the photocatalyst receives a photon having sufficient energy, i.e., equal to or greater than its band-gap energy (E_g), one of the electrons on its valence band (VB) can be excited enough to move to the conduction band (CB), by jumping the bandgap [20], leaving a positive-charged hole in the VB. This explains why the band-gap energy is such a crucial parameter in photocatalysis. In the electron-hole pair then created, both the electron and the hole are able to react with the species of the medium (i.e. water and/or oxygen) to form hydroxyl radicals (OH•), which possess high oxidation power, and thus will react with the molecules to be degraded, if they are adsorbed on the surface of the photocatalyst. The detailed mechanism has been reported in our previous work [19]. The OH• radicals having a very strong oxidation power, they can lead to a partial or complete mineralization of the organic pollutants (i.e. dyes) in the water; transforming them into harmless molecules, such as H_2O, CO_2 or NO_3^- etc.

Classic mode

In order to highlight the importance of the fluid movement in the water purification process, a set of experiments has been carried out both in static mode and in dynamic mode. In the case of the photocatalysis in static mode, the ZnO NWs sample was simply put at the bottom of the dye polluted water solution without any turbulence as illustrated in figure 4a. In such case, the only movement agitating the particles in the liquid is the Brownian motion, which is the random motion of particles (i.e. dye molecules) suspended in the liquid, resulting from their collision with the fast-moving molecules in the fluid [21]. In the case of the photocatalysis in dynamic mode, the ZnO NWs sample was put at middle-height in the aqueous solution, and a magnetic stirring has been added to create fluid turbulences in the solution. It is worth noting that the distance between the UV lamp and the sample surface was maintained at 10 cm in both cases. The quantity of the polluted water was fixed at 30 mL. In order to ensure the same distance between the water surface and the sample (d0, UV light pass in the water), we changed the beaker form (Figure 4b). Here, the solution stirring can ensure a constant supply of pollutant molecules on the photocatalyst surface. The initial concentration of dye-polluted-water solution of each organic dye was fixed at 10 µM for all tests.

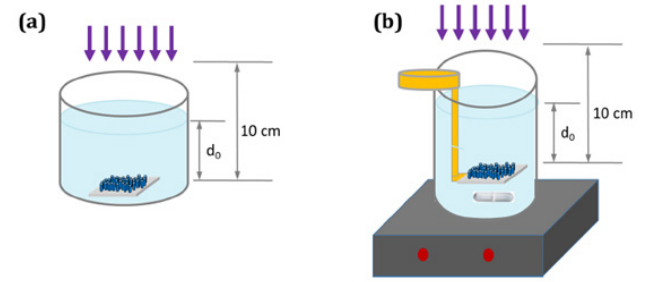

Figure 4: Experimental set-up illustrations for photocatalysis in (a) static mode and in (b) dynamic mode.

The photocatalysis process was monitored by UV-visible spectrometry, measured by using a sample of the solution taken every 15 min during the photodegradation process, allowing us to determine the photodegradation rate of the pollutant (i.e. dyes) in the water. Figure 5 shows the UV-vis spectra for the three dyes degradation both in static mode (Figures 5a, 5c and 5e) and in dynamic mode (Figures 5b, 5d, and 5f). We can note that, for each dye, the characteristic absorption peak (located at 665, 464 and 515 nm for the

molecules MB, MO and AR14, respectively) decreases faster during the photocatalysis under dynamic mode than under static mode. That means the photodegradation kinetic can be accelerated by the dynamic fluid regime due to a better contact between the pollutant molecules (i.e. dyes) and the semiconductor surface (i.e. ZnO NWs). This dynamic fluid regime can also maximize the removal of the formed reaction products from the catalyst surface. Furthermore, the magnetic stirring during the photocatalytic process can increase the oxygen supply in the aqueous solution, which can also improve the photocatalytic efficiency. In fact, as indicated in the photocatalysis mechanism presented in our previous work [19], the photo-generated holes of the VB can directly produce OH• radicals in the presence of H_2O by an oxidation reaction; while the photo-generated electrons of the CB can also indirectly produce OH• radicals via a reduction reaction in the presence of O_2, by producing the superoxide anions $O_2^{\bullet-}$. In other words, the photo-generated holes make the main contribution in water purification by photocatalysis due to the aqueous milieu being rich in H_2O molecules; but the dissolved oxygen in water can also contribute via the photo-generated electrons. On the contrary, in air purification by photocatalysis, the photo-generated electrons make the main contribution, as air is an oxygen-rich environment; but the humidity in the air can also contribute via the photo-generated holes. Thus, the photocatalytic efficiency increasing under the dynamic mode can be explained by two contributions: (1) a better contact between the pollutant molecules and the photocatalyst surface; (2) a bigger quantity of dissolved oxygen in water carried by dynamic mode.

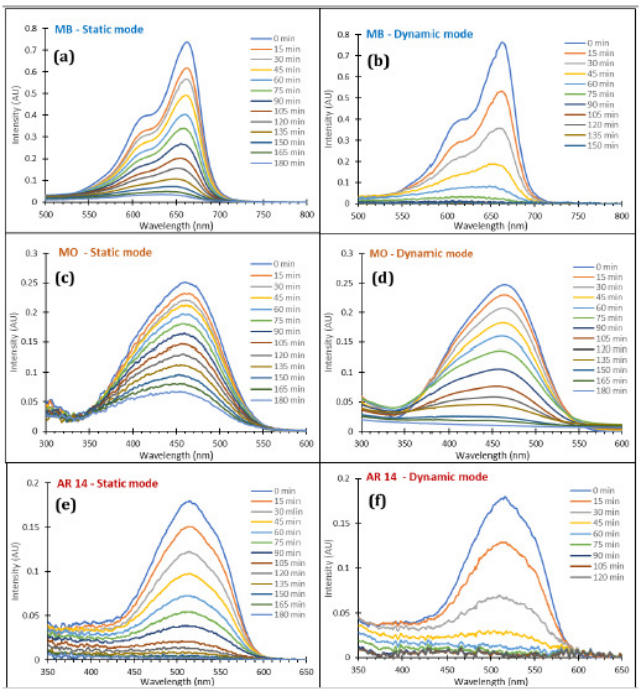

Figure 5: UV-vis absorption spectra evolution during ZnO NWs photocatalysis of the three dyes: (a) MB in static mode, (b) MB in dynamic mode, (c) MO in static mode, (d) MO in dynamic mode, (e) AR14 in static mode, and (f) AR14 in dynamic mode.

To compare directly the photodegradation efficiency, we use the degradation rate, X, which indicates the residual dye content in the aqueous solution, and is defined by the following equation:

$$X(\%) = \left(\frac{A_0 - A_T}{A_0}\right) \cdot \times 100\%$$

Where A_0 is the dye absorbance in the initial solution, at the maximum absorption wavelength of the appropriate dye before illumination, and A_t is the dye absorbance at time t during the photodegradation process.

Figure 6 shows a direct comparison of the influence of the fluid regime (static and dynamic) on the photodegradation rate for the three studied dyes. From figure 6, we can note that the photocatalysis efficiency of the ZnO NWs has been considerably improved for all of the three dyes degradation. In fact, the photodegradation rate has been improved at the beginning stage of the photocatalysis process in the dynamic operation mode, leading to a faster achievement of a (quasi) complete degradation of the organic dyes, even for MO dye, which is one of the most difficult dyes to be degraded compared to the other dyes such as MB and AR14. The MB and AR14 dyes reached total mineralization (with X = 100%) in less than 2 hours.

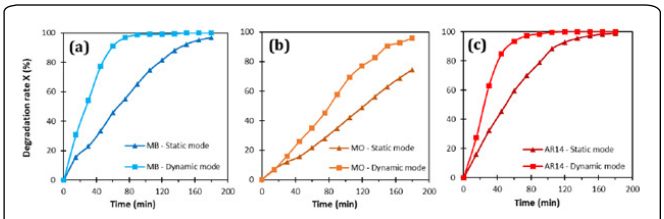

Figure 6: Photodegradation rate evolution of the three dye solutions: (a) MB, (b) MO, (c) AR14 under static mode and dynamic mode, respectively.

Note that the photodegradation time of 180 min is not a time limit; it was more of a pre-fixed time for all our photodegradation process study. It is important to highlight that the pollutant degradation have been taking place on the photocatalyst surface and the water depollution is not a simple adsorption phenomenon. In our previous work, we demonstrated that our photocatalyst (ZnO NWs) can be reused and maintain their efficiency without any surface treatment between each photocatalysis experiment [22]. The adsorption experience (not shown here) has also been carried out, and the degradation rate X remained at about 0% for 3 hours in the dark with the same pollutant concentration (10 μM) and polluted water solution volume (30 mL).

As demonstrated in our previous work [16], there is also a photolysis phenomenon during the photocatalysis process, especially for the MB solution. To take into account the photolysis effect, all photocatalytic measurements have been carried out in parallel with a reference solution without photocatalyst. The photolysis degradation rate is measured at about 40%, 4% and 12% for MB, MO, and AR14 respectively. For 180 min, we obtained the similar value both for static and dynamic operation modes due to the absence of photocatalyst in the solution.

Microfluidic mode

From the above paragraph, we can note that the photocatalysis process in bulk medium is fairly long. Few hours are often necessary to photodegrade the dye-polluted-water solutions, as shown in the literature, under approximatively the same experimental conditions [23, 24]. This time-consuming characteristic of the semiconductor based photocatalysis is notably due to the short diffusion length of the mass transfer [14, 15]. However, by using the microfluidic system, this flaw can be overcome, thanks to the small confined space in the microfluidic chamber. Moreover, by controlling the flow rate, the reaction-diffusion process can be optimized to obtain a rapid water purification device.

Beside the reaction-diffusion process improvement, the microfluidic chambers have two beneficial properties for the photocatalytic efficiency improvement. First, as the volume of liquid in the chamber is less important than in the beaker used for the classic mode, the light irradiation is less absorbed by the liquid above the sample, increasing the photon absorption by the photocatalyst, and thus, the photocatalytic efficiency. Second, the contact of the dye molecules with the nanowires is favored by the shape of the chamber, increasing the number of dye molecules adsorbed on the photocatalyst surface, where they can be degraded.

Due to the rapid photodegradation rate in microfluidic mode, the solution was monitored every minute instead of every 15 minutes in classic mode. Figure 7 shows a much higher photodegradation performance of the ZnO NWs integrated microfluidic device (Figure 3): only 5 minutes were necessary to reach total dye degradation for MB and AR14 and almost 80% of MO had been degraded after 7 min. To increase the general photocatalytic efficiency of the microfluidic system, this kind of microfluidic device can be connected in series. Owing to both to the fluid dynamics and the diffusion-reaction kinetics in microfluidic chamber, the dye concentration can be reduced very quickly. Moreover, we would like to highlight that the microfluidic chamber is recyclable without any treatment after each photodegradation experience, except one pure water pass.

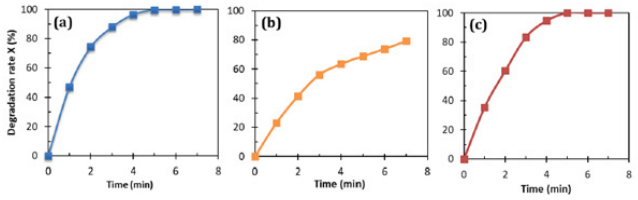

Figure 7: Photodegradation rate evolution of the three dye solutions: (a) MB, (b) MO, (c) AR14 under microfluidic mode, respectively.

Conclusion

Homogeneous and high aspect ratio ZnO nanowire arrays have been synthesized by a low-cost method: hydrothermal technique. The good photocatalytic performance of the ZnO NWs has been demonstrated both in static mode and in dynamic mode, the later exhibiting an enhanced photocatalytic efficiency due to the creation of fluid turbulences in the dye-polluted-water solutions. Two main contributions can be cited for this photocatalytic efficiency enhancement: the better contact between the dye molecules and the ZnO NWs surface; and the larger quantity of hydroxyl radicals produced in the aqueous solution by the increased oxygen supply. To overcome the time-consuming flaw of the classical photocatalysis concept, due to the short diffusion length of the mass transfer during the pollutant degradation process, a ZnO-NWs-integrated microfluidic chamber has been fabricated. This micro-reactor allowed to significantly shorten the water purification process from two – three hours to only a few minutes, using the combined effect of a better optimization of the reaction-diffusion process, an increased light absorption, and a better contact between the photocatalyst and the dye molecules. These simply designed micro-reactor chambers allow to consider the further development of highly efficient photocatalytic micro-reactors for water depollution, using ZnO NWs. For future work, a study of a high flow rate with low-pressure microfluidic reactor is ongoing. Furthermore, the ZnO NWs will be integrated directly by *in-situ* growth inside the microfluidic chamber.

Conflict of Interest

The authors declare no conflict of interest.

References

1. Shannon MA, Bohn PW, Elimelech M, Georgiadis JG, Mariñas BJ, et al. 2008. Science and technology for water purification in the coming decades. *Nature* 452: 301-310. https://doi.org/10.1038/nature06599
2. Stackelberg PE, Gibs J, Furlong ET, Meyer MT, Zaugg SD, et al. 2007. Efficiency of conventional drinking-water-treatment processes in removal of pharmaceuticals and other organic compounds. *Sci Total Environ* 377(2-3): 255-272. https://doi.org/10.1016/j.scitotenv.2007.01.095
3. Ni M, Leung MK, Leung DY, Sumathy KA. 2007. Review and recent developments in photocatalytic water-splitting using TiO_2 for hydrogen production. *Renew Sust Energ Rev* 11(3): 401-425. https://doi.org/10.1016/j.rser.2005.01.009
4. Ohno T, Bai L, Hisatomi T, Maeda K, Domen K. 2012. Photocatalytic water splitting using modified GaN:ZnO solid solution under visible light: long-time operation and regeneration of activity. *J Am Chem Soc* 134(19): 8254-8259. https://doi.org/10.1021/ja302479f
5. Daneshvar N, Salari D, Khataee A. 2004. Photocatalytic degradation of azo dye acid red 14 in water on ZnO as an alternative catalyst to TiO_2. *J Photochem Photobiol A Chem* 162(2-3): 317-322. https://doi.org/10.1016/S1010-6030(03)00378-2
6. Drobne D. 2018. Spotlighting CLH report for TiO_2: nano-safety perspective. *Chem Eng J* 340: 192–195. https://doi.org/10.1016/j.cej.2018.01.007
7. Report of WHO-IARC Working Group on the Evaluation of Carcinogenic Risks to Humans in Lyon FRANCE. IARC monographs on the evaluation of carcinogenic risks to humans. WHO, France. 2010.
8. Li Z, Yang R, Yu M, Bai F, Li C, et al. 2008. Cellular level biocompatibility and biosafety of ZnO nanowires. *J Phys Chem C* 112(51): 20114-20117. https://doi.org/10.1021/jp808878p
9. Gargas DJ, Gao H, Wang H, Yang P. 2011. High quantum efficiency of band-edge emission from ZnO nanowires. *Nano lett* 11(9): 3792-3796. https://doi.org/10.1021/nl201850k

10. Ong BS, Li C, Li Y, Wu Y, Loutfy R. 2007. Stable, solution-processed, high-mobility ZnO thin-film transistors. *J Am Chem Soc* 129(10): 2750-2751. https://doi.org/10.1021/ja068876e

11. Reimer T, Paulowicz I, Röder R, Kaps S, Lupan O, et al. 2014. Single step integration of ZnO nano-and microneedles in Si trenches by novel flame transport approach: whispering gallery modes and photocatalytic properties. *ACS Appl Mater Interfaces* 6(10): 7806-7815. https://doi.org/10.1021/am5010877

12. Joswig JO, Roy S, Sarkar P, Springborg M. 2002. Stability and bandgap of semiconductor clusters. *Chem Phys Lett* 365(1-2): 75-81. https://doi.org/10.1016/S0009-2614(02)01421-5

13. Özgür Ü, Alivov YI, Liu C, Teke A, Reshchikov MA, et al. 2005. A comprehensive review of ZnO materials and devices. *J Appl Phys* 98(4): 041301. https://doi.org/10.1063/1.1992666

14. Van Gerven T, Mul G, Moulijn J, Stankiewicz A. 2007. A review of intensification of photocatalytic processes. *Chem Eng Process* 46(9): 781-789. https://doi.org/10.1016/j.cep.2007.05.012

15. Lin H, Valsaraj KT. 2005. Development of an optical fiber monolith reactor for photocatalytic wastewater treatment. *J Appl Electrochem* 35: 699-708. https://doi.org/10.1007/s10800-005-1364-x

16. Habba YG, Capochichi-Gnambodoe M, Serairi L, Leprince-Wang Y. 2016. Enhanced photocatalytic activity of ZnO nanostructure for water purification. *Phys Status Solidi B* 253(8): 1480-1484. https://doi.org/10.1002/pssb.201600031

17. Chevalier-César C, Capochichi-Gnambodoe M, Leprince-Wang Y. 2014. Growth mechanism study of ZnO nanowire arrays via hydrothermal method. *Appl Phys A* 115: 953-960. https://doi.org/10.1007/s00339-013-7908-8

18. Jang ES, Won JH, Hwang SJ, Choy JH. 2006. Fine tuning of the face orientation of ZnO crystals to optimize their photocatalytic activity. *Adv Mater* 18(24): 3309-3312. https://doi.org/10.1002/adma.200601455

19. Habba YG, Capochichi-Gnambodoe M, Leprince-Wang Y. 2017. Enhanced photocatalytic activity of iron-doped ZnO nanowires for water purification. *Appl Sci* 7(11): 1185. https://doi.org/10.3390/app7111185

20. Mills A, Le Hunte S. 1997. An overview of semiconductor photocatalysis. *J Photochem Photobiol A Chem* 108(1): 1-35. https://doi.org/10.1016/S1010-6030(97)00118-4

21. Feynman R. 1964. The Brownian Movement. *The Feynman Lectures of Physics* 1: 41-45.

22. Le Pivert M, Poupart R, Capochichi-Gnambodoe M, Martin N, Leprince-Wang Y. 2019. Direct growth of ZnO nanowires on civil engineering materials: smart materials for supported photodegradation. *Microsyst Nanoeng* 5: 57. https://doi.org/10.1038/s41378-019-0102-1

23. Baruah S, Pal SK, Dutta J. 2012. Nanostructured zinc oxide for water treatment. *Nano Sci Technol Asia* 2(2): 90-102. https://doi.org/10.2174/2210681211202020090

24. Lavčević ML, Penava A. 2017. ZnO nanostructured photocatalysts for water treatment applications. *Croat J Food Sci Technol* 9(2): 192-197. https://doi.org/10.17508/CFST.2017.9.2.17